

Electronic Supplementary Information

The naphthalimide-derived hypochlorite fluorescent probe from ACQ to AIE effect transformation

Chenggong Xu,^a Tian Wu,^a Lizheng Duan,^a and Yanmei Zhou^{*a,b}

^aHenan Joint International Research Laboratory of Environmental Pollution Control
Materials, College of Chemistry and Chemical Engineering, Henan University,
Kaifeng, 475004, China

^bState Key Laboratory of Fine Chemicals, Dalian University of Technology, Dalian,
116024, China

*Corresponding author: Tel: +86-371-23881589; Fax: +86-371-23881589

E-mail address: zhouyanmei@henu.edu.cn

Table of Contents	
Contents	Page
Experimental section	S-3
Table S1. Comparison of the related fluorescent probes for ClO ⁻	S-6
Fig S1. MS monitoring the reaction between Probe A and ClO ⁻	S-7
Fig S2. MS monitoring the reaction between Probe B and ClO ⁻	S-7
Fig S3. Cytotoxicity study	S-7
Fig S4. Confocal fluorescence images of HepG2 cells	S-8
Fig S5. The transmission electron microscope analysis	S-8
Fig S6. Spectral analysis in different solvent systems	S-9
Fig S7. DFT calculations	S-9
Fig S8. Selective study of Probe B for ClO ⁻	S-9
Fig S9. Fluorescence intensity ratio study	S-10
Fig S10. Mass spectra of Compound 1	S-10
Fig S11. ¹ H NMR of Compound 1	S-11
Fig S12. ¹³ C NMR of Compound 1	S-12
Fig S13. Mass spectra of Probe A	S-12
Fig S14. ¹ H NMR of Probe A	S-13
Fig S15. ¹³ C NMR of Probe A	S-14
Fig S16. Mass spectra of Probe B	S-14
Fig S17. ¹ H NMR of Probe B	S-15
Fig S18. ¹³ C NMR of Probe B	S-16
References	S-16

Experimental section

Materials and apparatus. The experimental chemicals obtained from suppliers were not further purified before use. The nuclear magnetic resonance (NMR) spectra were recorded from a Bruker AVANCE III HD 400 MHz and Bruker AVANCE NEO 500 MHz spectrometer instruments. The mass spectrometry (MS) spectra were performed from a Bruker Amazon SL instrument. The U-4100 spectrophotometer and Edinburgh FS5 were used to the collection of UV-vis absorption and fluorescence spectra. The laser scanning confocal microscope (Olympus FV3000) was employed to obtain the cell images.

Synthesis and characterization. Three naphthalimide-derived compounds named Compound 1, Probe A and Probe B were synthesized according to the procedures shown in Scheme 1.

The details of Compound 1. The synthesis process of Compound 1 was referred to the published articles.^[1-3] ¹H NMR (400 MHz, Chloroform-*d*) δ 8.62 (dd, $J = 7.3$, 1.2 Hz, 1H), 8.51 (dd, $J = 8.5$, 1.2 Hz, 1H), 8.37 (d, $J = 7.8$ Hz, 1H), 8.00 (d, $J = 7.9$ Hz, 1H), 7.81 (dd, $J = 8.5$, 7.3 Hz, 1H), 4.17-4.08 (m, 2H), 1.83-1.69 (m, 2H), 1.02 (t, $J = 7.4$ Hz, 3H). ¹³C NMR (101 MHz, Chloroform-*d*) δ 163.39, 163.36, 132.94, 131.82, 131.00, 130.93, 130.33, 130.00, 128.70, 127.93, 122.95, 122.09, 42.04, 21.35, 11.55. ESI-MS: m/z , calcd: 317.01, found: 318.16 ($[M + H]^+$).

The details of Probe A. In a 100 mL round bottom flask, Compound 1 (63.4 mg, 0.2 mmol), sodium thiomethoxide (84.1 mg, 0.24 mmol), K₂CO₃ (27.6 mg, 0.2 mmol) and DMF (60 mL) were added sequentially, and heated at 90°C under N₂ for 6 h.

After the reaction completed, the mixture was poured into 300 mL ice water and the precipitate was collected, and the Probe A was purified by silica gel column chromatography (petroleum ether : dichloromethane = 2 : 1). ¹H NMR (400 MHz, Chloroform-*d*) δ 8.60 (d, *J* = 7.2 Hz, 1H), 8.51-8.42 (m, 2H), 7.77-7.67 (m, 1H), 7.42 (dd, *J* = 7.9, 1.7 Hz, 1H), 4.18-4.09 (m, 2H), 2.68 (d, *J* = 1.7 Hz, 3H), 1.77 (h, *J* = 7.6 Hz, 2H), 1.01 (t, *J* = 7.5 Hz, 3H). ¹³C NMR (126 MHz, Chloroform-*d*) δ 163.98, 163.96, 146.14, 131.30, 130.72, 129.44, 128.81, 127.96, 126.42, 123.07, 120.87, 118.72, 41.88, 21.40, 14.83, 11.55. ESI-MS: *m/z*, calcd: 285.08, found: 285.88 ([M + H]⁺).

The details of Probe B. In a 100 mL round bottom flask, Compound 1 (63.4 mg, 0.2 mmol), (4-methylsulfanylphenyl)boronic acid (40.3 mg, 0.24 mmol), K₂CO₃ (27.6 mg, 0.2 mmol), Pd(PPh₃)₄ (11.6 mg, 0.01 mmol) and EtOH (60 mL) were added sequentially, and refluxed at 80°C under N₂ for 8 h. After that, the solvent was removed by rotary evaporation, and the Probe B was purified by silica gel column chromatography (petroleum ether : dichloromethane = 2 : 1). ¹H NMR (400 MHz, DMSO-*d*₆) δ 8.54-8.47 (m, 2H), 8.24 (dd, *J* = 8.5, 1.2 Hz, 1H), 7.87-7.73 (m, 2H), 7.54-7.43 (m, 4H), 4.06-3.98 (m, 2H), 2.58 (s, 3H), 1.67 (h, *J* = 7.5 Hz, 2H), 0.94 (t, *J* = 7.4 Hz, 3H). ¹³C NMR (101 MHz, Chloroform-*d*) δ 164.29, 164.09, 146.23, 139.58, 135.32, 132.43, 131.15, 130.80, 130.28, 129.99, 127.71, 126.81, 126.31, 122.97, 121.74, 41.97, 21.42, 15.57, 11.55. ESI-MS: *m/z*, calcd: 361.11, found: 362.24 ([M + H]⁺).

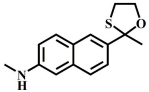
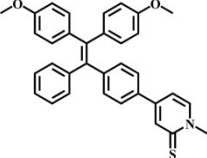
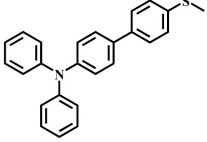
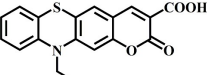
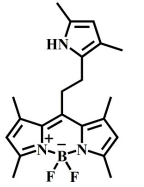
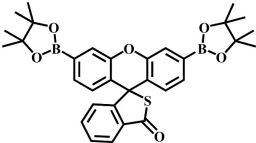
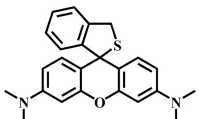
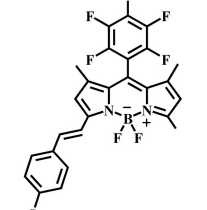
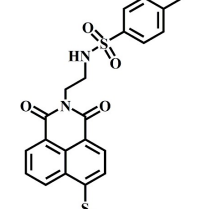
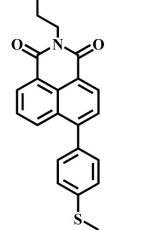
Solution preparation and spectral analysis. The stock solutions of Probe A

and Probe B (1 mM) were prepared with N,N-Dimethylformamide (DMF). The stock solutions of ClO^- and other analytes including H_2O_2 , $\bullet\text{OH}$, ONOO^- , MnO_4^- , $^1\text{O}_2$, O_2^- , NO_2^- , TBHP, DTBP, S^{2-} , SO_3^{2-} , Cys, Hcy, GSH, $\text{NH}_3 \cdot \text{H}_2\text{O}$, K^+ , Na^+ , Ca^{2+} and Mg^{2+} were prepared in deionized water. All the spectra experiments were performed in DMF-PBS buffer solution (10 mM, pH = 7.4, 1/99, v/v) at room temperature.

Construction and application of test paper. The filter paper strips were firstly soaked in a dichloromethane solution containing 10 μM Probe B, then took it out and dried in natural, and the ClO^- test paper was successfully manufactured. Afterwards, various kinds of analytes and different concentrations of ClO^- were carefully sprayed on the test paper, and the fluorescence color change can be observed with naked eyes directly under 365 nm UV light.

Cytotoxicity analysis and live cell imaging. In order to ensure that the Probe B can be successfully applied to live cell imaging, its cytotoxicity was first investigated with 3-(4,5-dimethyl-2-thiazolyl)-2,5-diphenyltetrazolium bromide (MTT) assay, and the details were referred to the published literatures. Subsequently, in the atmosphere of 37°C with 5% CO_2 , the HepG2 cells were cultured with different concentrations of ClO^- ranging from 0 to 60 μM for 30 min, and then washed with PBS buffer solution for 3 times. Afterwards, the cells were incubated with 10 μM Probe B for another 30 min. Under 405 nm excitation, the confocal fluorescence imaging in blue and green channels were collected in the range of 420-440 nm and 480-520 nm respectively.

Table S1. Comparison of the related fluorescent probes for ClO⁻.

Probes	Solution	FL change	Em shift	LOD	AIE	Ref.
	50% EtOH	Turn-on	-	16.6 nM	-	[4]
	-	Turn-on	-	92 nM	√	[5]
	50% DMF	Ratiometric	60 nm	16 nM	-	[6]
	-	Turn-on	-	16.1 nM	-	[7]
	10% EtOH	Turn-on	-	0.56 nM	-	[8]
	-	Turn-on	-	-	-	[9]
	0.1% DMF	Turn-on	-	-	-	[10]
	50% DMF	Ratiometric	32 nm	59 nM	-	[11]
	1% DMSO	Turn-off	-	120 nM	-	[12]
	1% DMF	Ratiometric	68 nm	20 nM	√	This work

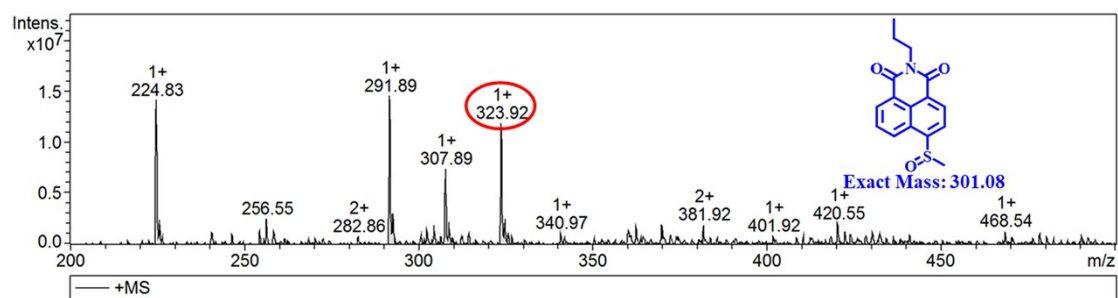


Fig S1. ESI mass spectrometry monitoring the reaction between Probe A and ClO⁻.

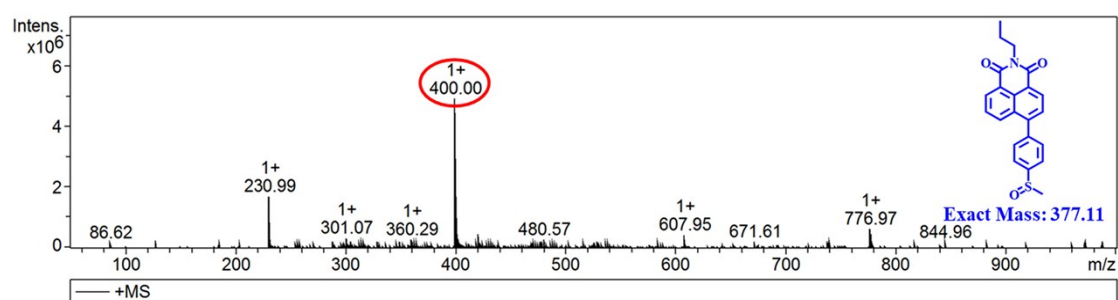


Fig S2. ESI mass spectrometry monitoring the reaction between Probe B and ClO⁻.

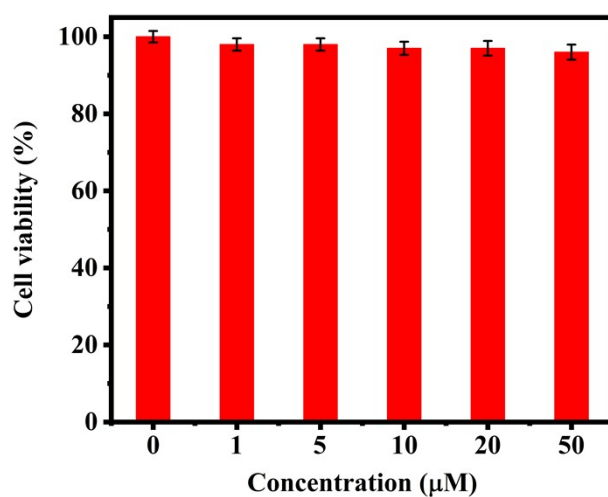


Fig S3. Survival rate of HepG2 cells after incubation with different concentrations of Probe B (0, 1, 5, 10, 20 and 50 µM) for 24 h.

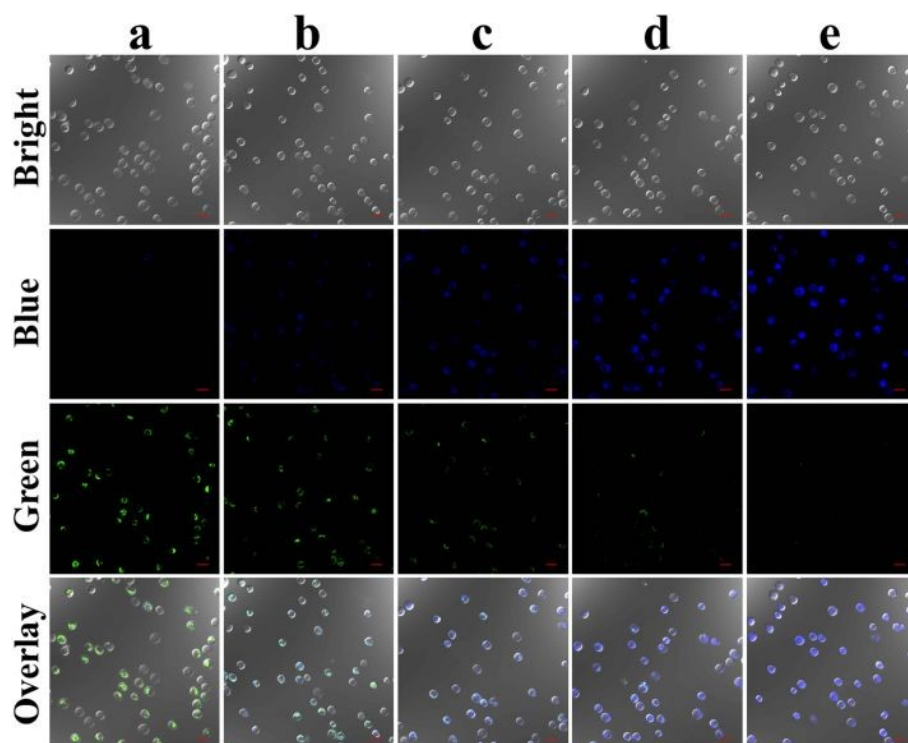


Fig S4. Confocal fluorescence images of HepG2 cells with Probe B (10 μM) after the pre-treatment with (a) 0 μM , (b) 10 μM , (c) 20 μM , (d) 40 μM and (e) 60 μM ClO^- for 30 min. Scale bar: 20 μm .

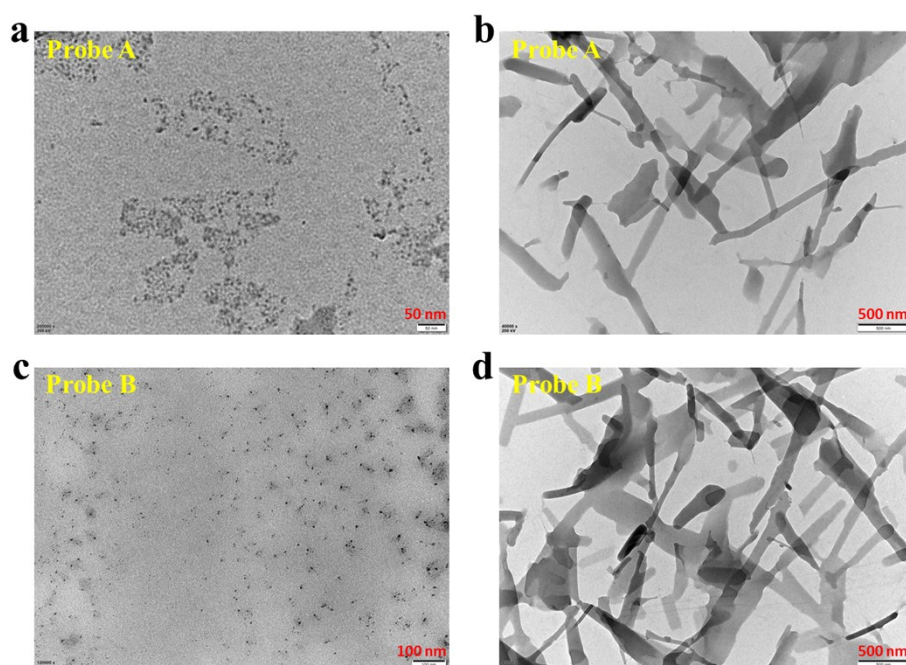


Fig S5. The TEM images of Probe A and Probe B in (a, c) 100% EtOH and (b, d) a solvent system (EtOH: H_2O = 1: 99 v/v) after drying on copper mesh.

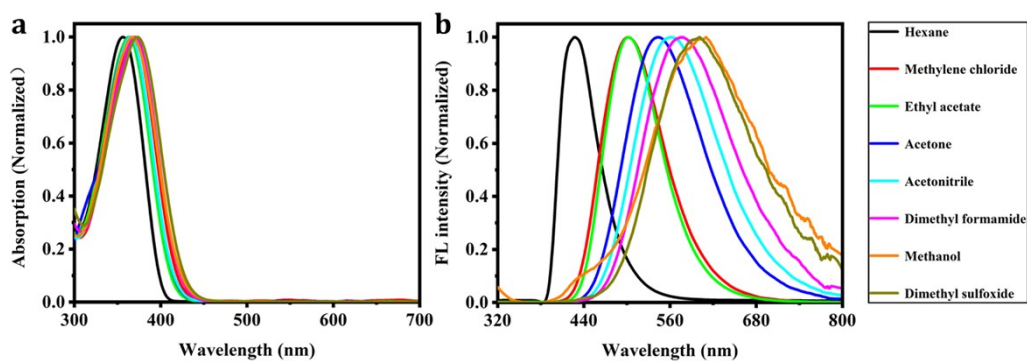


Fig S6. The normalized (a) absorption and (b) fluorescence spectra of Probe B in different solvents.

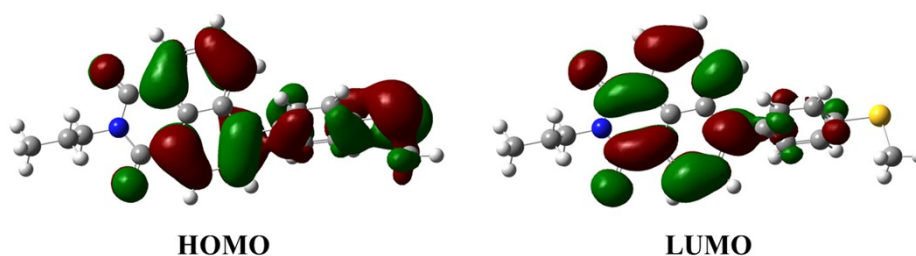


Fig S7. DFT calculations about HOMO and LUMO distributions of Probe B.

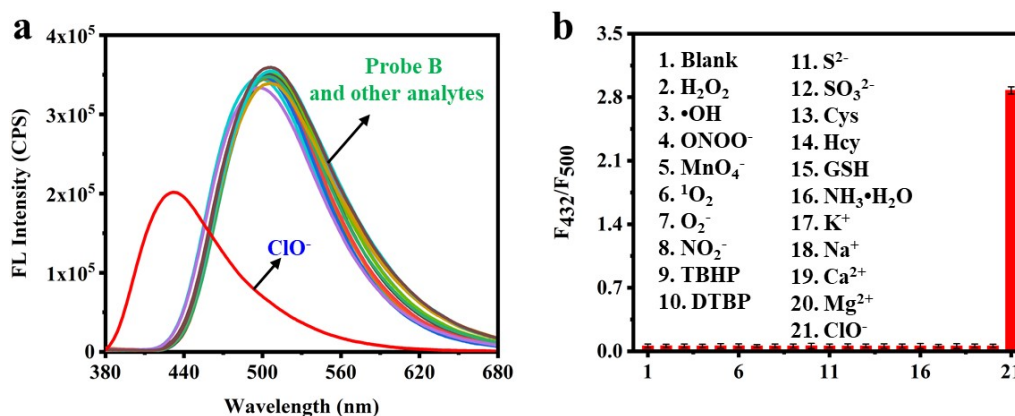


Fig S8. (a) The fluorescence spectra and (b) fluorescence intensity ratio (F_{432}/F_{500}) of Probe B (10 μM) after the addition of different kinds of analytes (500 μM). (1) Blank, (2) H_2O_2 , (3) $\bullet\text{OH}$, (4) ONOO^- , (5) MnO_4^- , (6) $^1\text{O}_2$, (7) O_2^- , (8) NO_2^- , (9) TBHP, (10) DTBP, (11) S^{2-} , (12) SO_3^{2-} , (13) Cys, (14) Hcy, (15) GSH, (16) $\text{NH}_3\cdot\text{H}_2\text{O}$, (17) K^+ , (18) Na^+ , (19) Ca^{2+} , (20) Mg^{2+} and (21) ClO^- (100 μM).

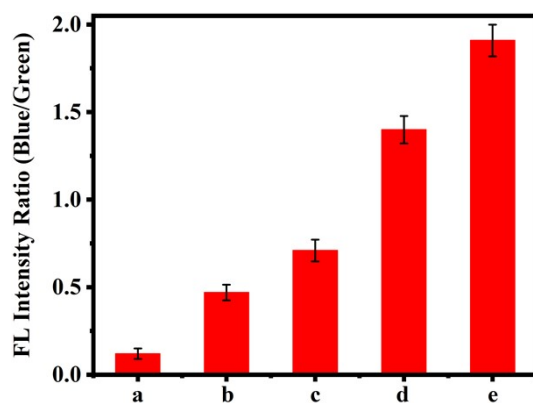


Fig S9. Fluorescence intensity ratio ($F_{\text{blue}}/F_{\text{green}}$) obtained from images (a-e) in Fig 5.

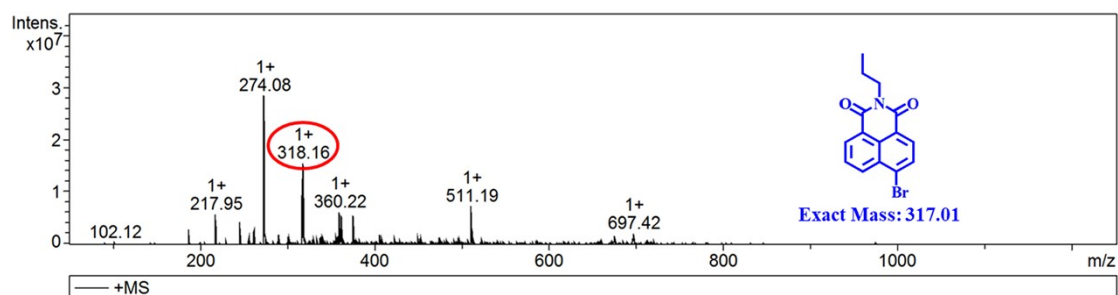


Fig S10. ESI mass spectra of Compound 1. ESI-MS: m/z , calcd: 317.01, found: 318.16 ($[M + H]^+$).

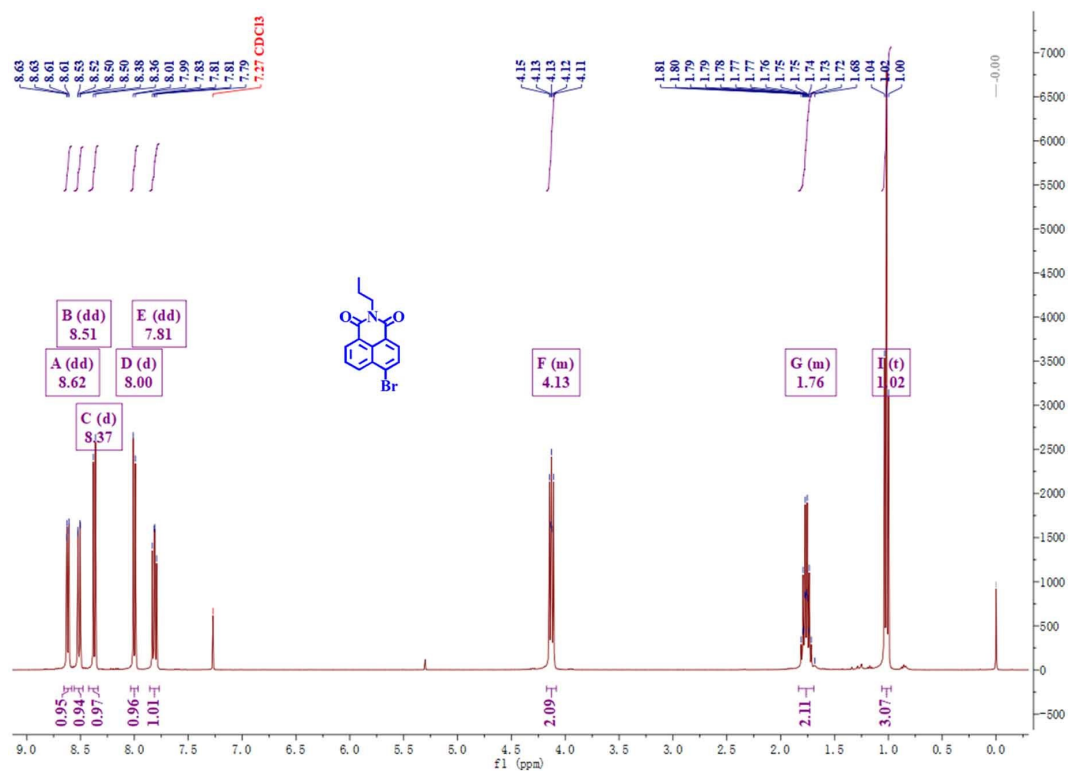


Fig S11. ^1H NMR of Compound 1 in CDCl_3 . ^1H NMR (400 MHz, Chloroform-*d*) δ 8.62 (dd, $J = 7.3, 1.2$ Hz, 1H), 8.51 (dd, $J = 8.5, 1.2$ Hz, 1H), 8.37 (d, $J = 7.8$ Hz, 1H), 8.00 (d, $J = 7.9$ Hz, 1H), 7.81 (dd, $J = 8.5, 7.3$ Hz, 1H), 4.17-4.08 (m, 2H), 1.83-1.69 (m, 2H), 1.02 (t, $J = 7.4$ Hz, 3H).

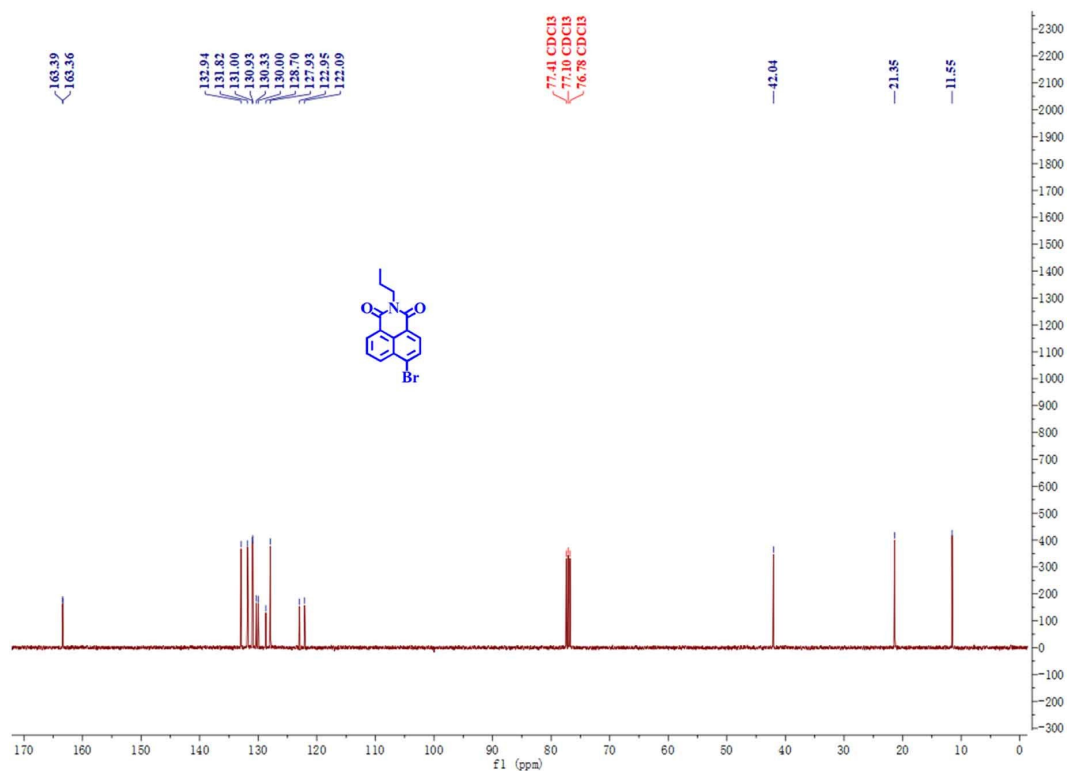


Fig S12. ¹³C NMR of Compound 1 in CDCl₃. ¹³C NMR (101 MHz, Chloroform-*d*) δ 163.39, 163.36, 132.94, 131.82, 131.00, 130.93, 130.33, 130.00, 128.70, 127.93, 122.95, 122.09, 42.04, 21.35, 11.55.

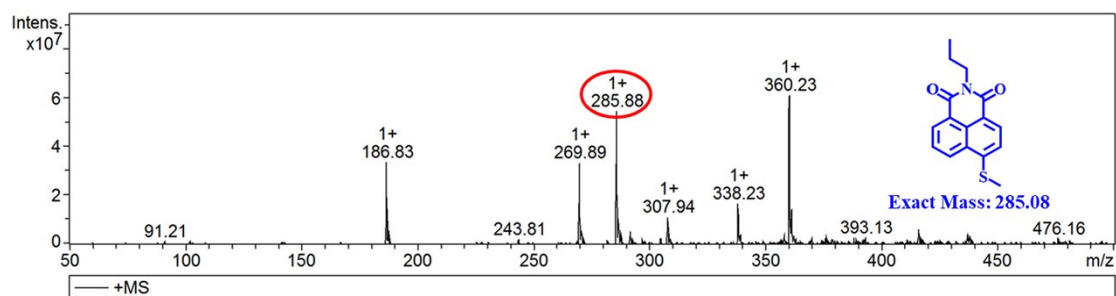


Fig S13. ESI mass spectra of Probe A. ESI-MS: m/z , calcd: 285.08, found: 285.88 ([M + H]⁺).

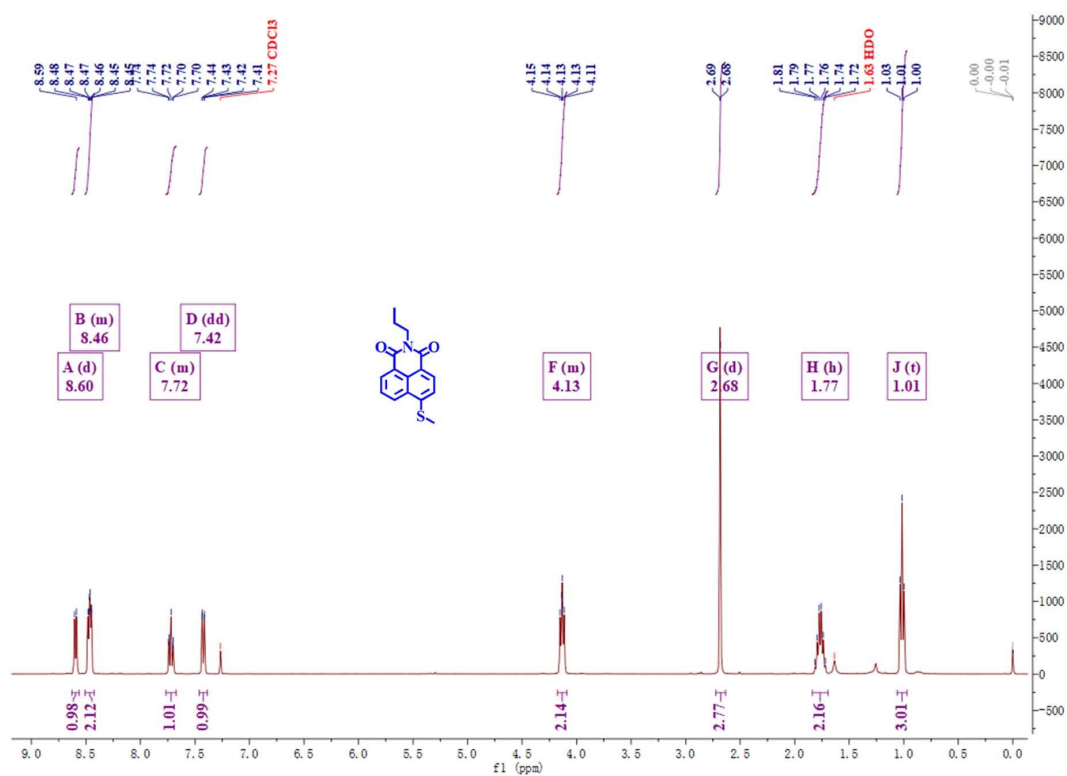


Fig S14. ^1H NMR of Probe A in CDCl_3 . ^1H NMR (400 MHz, Chloroform-*d*) δ 8.60 (d, $J = 7.2$ Hz, ^1H), 8.51-8.42 (m, 2H), 7.77-7.67 (m, ^1H), 7.42 (dd, $J = 7.9, 1.7$ Hz, ^1H), 4.18-4.09 (m, 2H), 2.68 (d, $J = 1.7$ Hz, 3H), 1.77 (h, $J = 7.6$ Hz, 2H), 1.01 (t, $J = 7.5$ Hz, 3H).

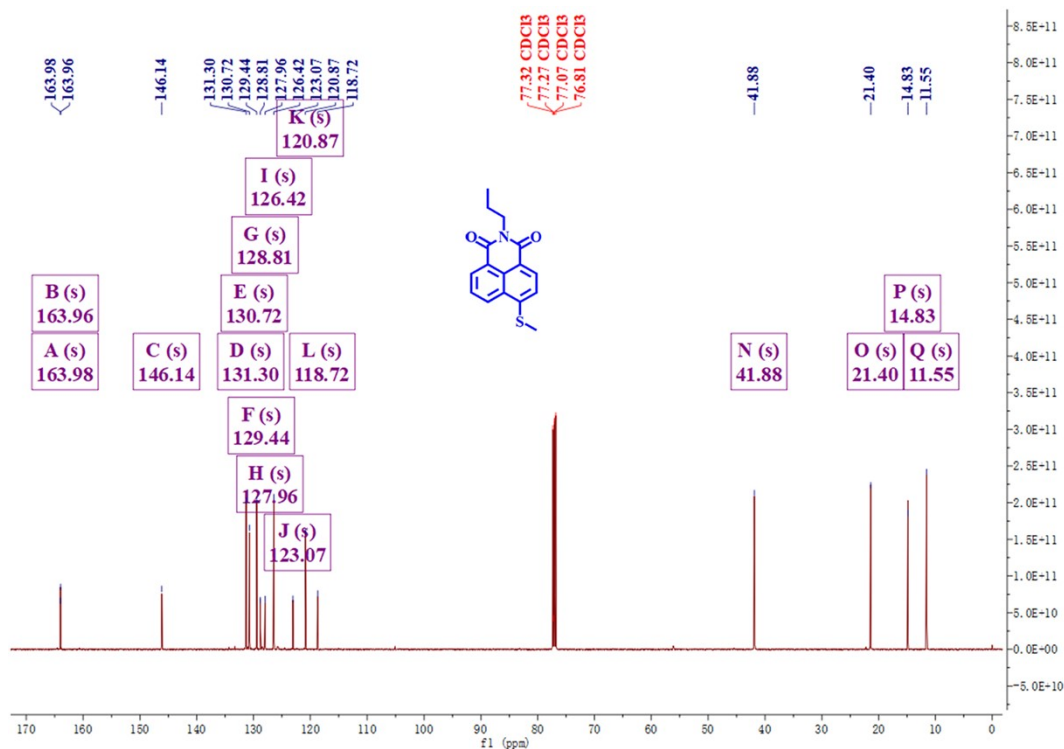


Fig S15. ^{13}C NMR of Probe A in CDCl_3 . ^{13}C NMR (126 MHz, Chloroform-*d*) δ 163.98, 163.96, 146.14, 131.30, 130.72, 129.44, 128.81, 127.96, 126.42, 123.07, 120.87, 118.72, 41.88, 21.40, 14.83, 11.55.

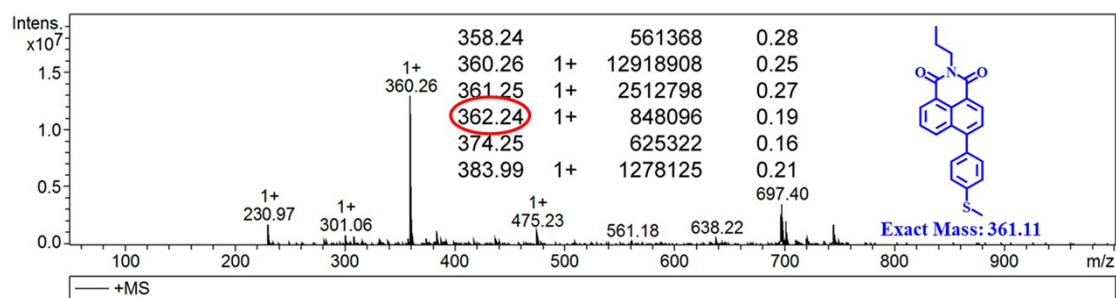


Fig S16. ESI mass spectra of Probe B. ESI-MS: m/z , calcd: 361.11, found: 362.24 ($[\text{M} + \text{H}]^+$).

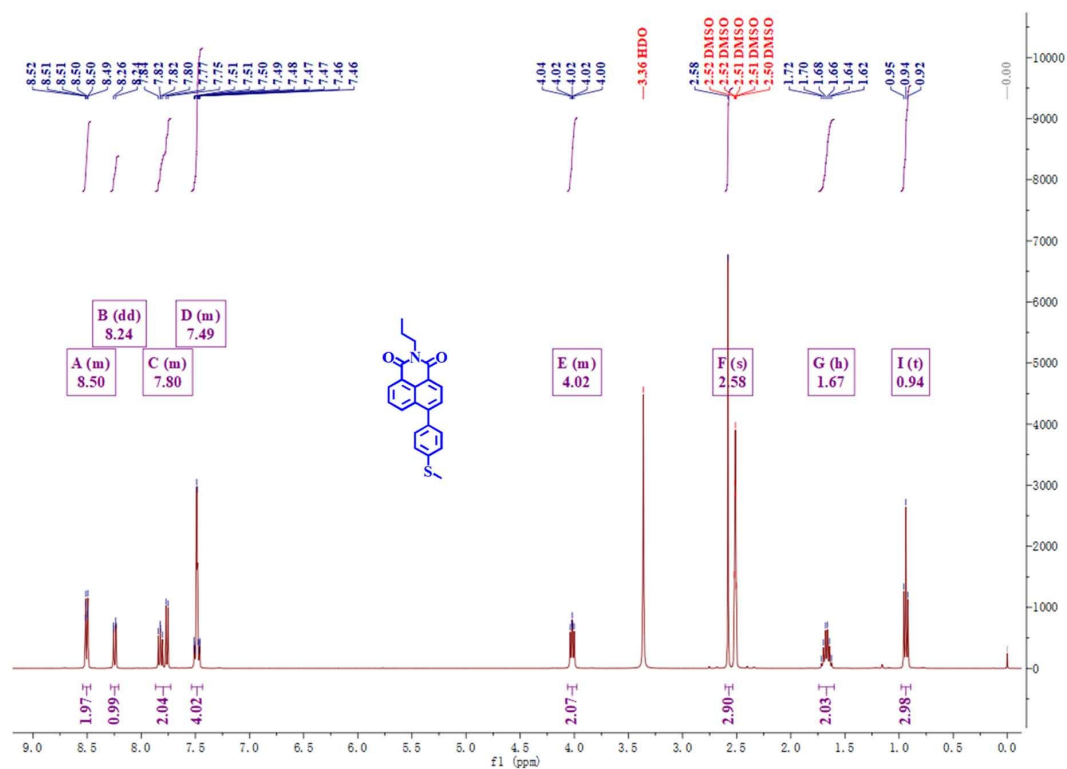


Fig S17. ^1H NMR of Probe B in $\text{DMSO-}d_6$. ^1H NMR (400 MHz, $\text{DMSO-}d_6$) δ 8.54-8.47 (m, 2H), 8.24 (dd, $J = 8.5, 1.2$ Hz, 1H), 7.87-7.73 (m, 2H), 7.54-7.43 (m, 4H), 4.06-3.98 (m, 2H), 2.58 (s, 3H), 1.67 (h, $J = 7.5$ Hz, 2H), 0.94 (t, $J = 7.4$ Hz, 3H).

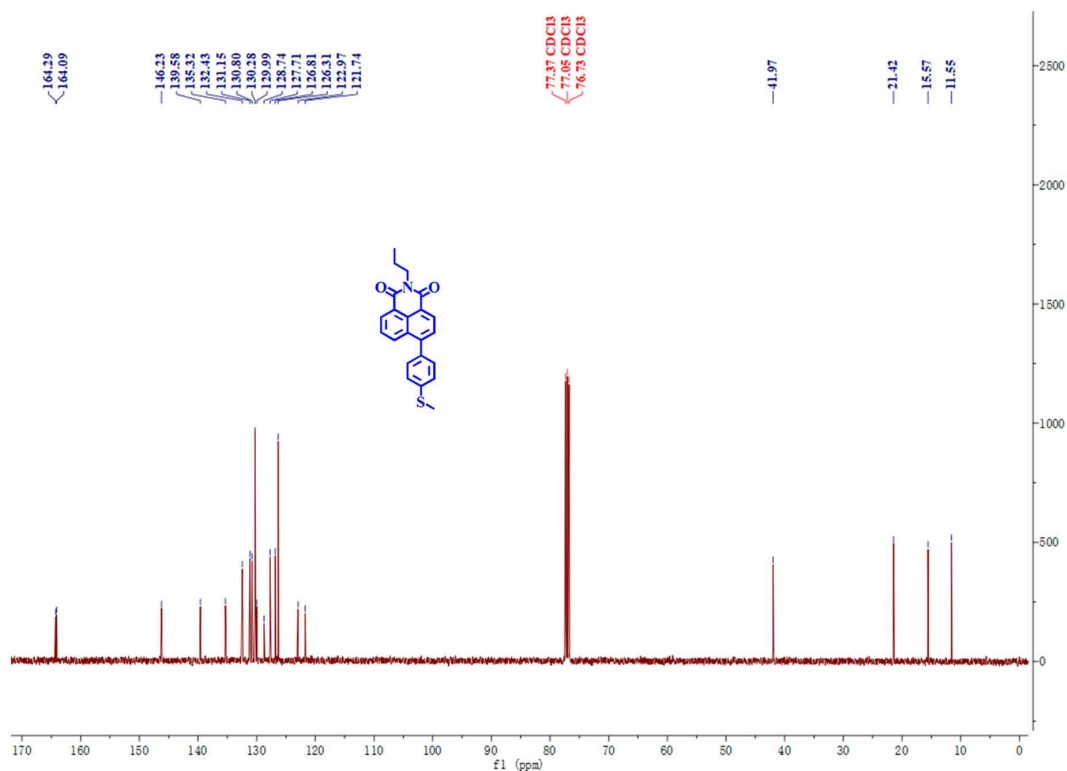


Fig S18. ^{13}C NMR of Probe B in CDCl_3 . ^{13}C NMR (101 MHz, Chloroform-*d*) δ 164.29, 164.09, 146.23, 139.58, 135.32, 132.43, 131.15, 130.80, 130.28, 129.99, 128.74, 127.71, 126.81, 126.31, 122.97, 121.74, 41.97, 21.42, 15.57, 11.55.

References

1. N. Jiang, B. Wang, G. Zheng, Y. Xing, C. Wang and Q. Wang. A fluorescent probe for specific lysosome imaging in cells. *Anal. Methods.*, 2017, 9, 2788-2790.
2. F. Liu, P. Tang, R. Ding, L. Liao, L. Wang, M. Wang and J. Wang. A glycosylation strategy to develop a low toxic naphthalimide fluorescent probe for the detection of Fe^{3+} in aqueous medium. *Dalton T.*, 2017, 46, 7515-7522.
3. B. Dong, X. Song, C. Wang, X. Kong, Y. Tang and W. Lin. Dual Site-Controlled and Lysosome-Targeted Intramolecular Charge Transfer-Photoinduced Electron Transfer-Fluorescence Resonance Energy Transfer Fluorescent Probe for Monitoring pH Changes in Living Cells. *Anal. Chem.*, 2016, 88, 4085-4091.
4. L. Yuan, L. Wang, B. K. Agrawalla, S. Park, H. Zhu, B. Sivaraman, J. Peng, Q. Xu, and Y. Chang. Development of Targetable Two-Photon Fluorescent Probes to Image Hypochlorous Acid in Mitochondria and Lysosome in Live Cell and

- Inflamed Mouse Model. *J Am Chem Soc.*, 2015, 137, 5930-5938.
5. X. Dong, G. Zhang, J. Shi, Y. Wang, M. Wang, Q. Peng and D. Zhang. A highly selective fluorescence turn-on detection of ClO^- with 1-methyl-1,2-dihydropyridine-2-thione unit modified tetraphenylethylene. *Chem Commun.*, 2017, 53, 11654-11657.
 6. Y. Lou, C. Wang, S. Chi, S. Li, Z. Mao and Z. Liu. Construction of a two-photon fluorescent probe for ratiometric imaging of hypochlorous acid in alcohol-induced liver injury. *Chem Commun.*, 2019, 55, 12912-12915.
 7. J. Hou, B. Wang, Y. Zou, P. Fan, X. Chang, X. Cao, S. Wang and F. Yu. Molecular Fluorescent Probe for Imaging and Evaluation of Hypochlorite Fluctuations during Diagnosis and Therapy of Osteoarthritis in Cells and in Mice Model. *ACS Sens.*, 2020, 5, 1949-1958.
 8. H. Zhu, J. Fan, J. Wang, H. Mu and X. Peng. An “Enhanced PET”-Based Fluorescent Probe with Ultrasensitivity for Imaging Basal and Elesclomol-Induced HClO in Cancer Cells. *J Am Chem Soc.*, 2014, 136, 12820-12823.
 9. Q. Xu, K. Lee, S. Lee, K. M. Lee, W. Lee and J. Yoon. A Highly Specific Fluorescent Probe for Hypochlorous Acid and Its Application in Imaging Microbe-Induced HOCl Production. *J Am Chem Soc.*, 2013, 135, 9944-9949.
 10. S. Kenmoku, Y. Urano, H. Kojima and T. Nagano. Development of a Highly Specific Rhodamine-Based Fluorescence Probe for Hypochlorous Acid and Its Application to Real-Time Imaging of Phagocytosis. *J Am Chem Soc.*, 2007, 129, 7313-7318.
 11. C. Duan, M. Won, P. Verwilt, J. Xu, H. S. Kim, L. Zeng and J. S. Kim. In Vivo Imaging of Endogenously Produced HClO in Zebrafish and Mice Using a Bright, Photostable Ratiometric Fluorescent Probe. *Anal. Chem.*, 2019, 91, 4172-4178.
 12. Q. Xia, X. Wang, Y. Liu, Z. Shen, Z. Ge, H. Huang, X. Li and Y. Wang. An endoplasmic reticulum-targeted two-photon fluorescent probe for bioimaging of HClO generated during sleep deprivation. *Spectrochim Acta A Mol Biomol Spectrosc.*, 2020, 229, 117992.